

Age of Information: Can CR-NOMA Help?

Zhiguo Ding, *Fellow, IEEE*, Robert Schober, *Fellow, IEEE*, and H. Vincent Poor,
Life Fellow, IEEE

Abstract

The aim of this paper is to exploit cognitive-ratio inspired NOMA (CR-NOMA) transmission to reduce the age of information in wireless networks. In particular, two CR-NOMA transmission protocols are developed by utilizing the key features of different data generation models and applying CR-NOMA as an add-on to a legacy orthogonal multiple access (OMA) based network. The fact that the implementation of CR-NOMA causes little disruption to the legacy OMA network means that the proposed CR-NOMA protocols can be practically implemented in various communication systems which are based on OMA. Closed-form expressions for the AoI achieved by the proposed NOMA protocols are developed to facilitate performance evaluation, and asymptotic studies are carried out to identify two benefits of using NOMA to reduce the AoI in wireless networks. One is that the use of NOMA provides users more opportunities to transmit, which means that the users can update their base station more frequently. The other is that the use of NOMA can reduce access delay, i.e., the users are scheduled to transmit earlier than in the OMA case, which is useful to improve the freshness of the data available in the wireless network.

I. INTRODUCTION

In order to support the services envisioned for the sixth generation (6G) mobile network, such as ultra massive machine type communications (umMTC) and enhanced ultra-reliable low latency communications (eURLLC), it is critical to ensure the freshness of the data collected in the network [1]–[5]. For example, as an important application of umMTC, smart cities require the data for air quality control, traffic management, and critical infrastructure monitoring to be timely and frequently collected [6], [7]. We note that the conventional performance evaluation metrics, such as the ergodic data rate and bit error probability, are not adequate for measuring the freshness of the data available in the network, which motivates a recently developed metric, termed the age

Z. Ding and H. V. Poor are with the Department of Electrical and Computer Engineering, Princeton University, Princeton, NJ 08544, USA. Z. Ding is also with the School of Electrical and Electronic Engineering, the University of Manchester, Manchester, UK (email: zhiguo.ding@manchester.ac.uk, poor@princeton.edu). R. Schober is with the Institute for Digital Communications, Friedrich-Alexander-University Erlangen-Nurnberg (FAU), Germany (email: robert.schober@fau.de).

of information (AoI). In particular, the AoI is defined as the time elapsed between the generation time and the received time of a successfully delivered update, and the AoI achievable for single-user transmission has been rigorously characterized in [1], [2]. For energy constrained wireless networks, such as sensor networks, the use of energy harvesting is important, and the impact of energy harvesting on the AoI has been studied in [8]. For the scenario with correlated information from multiple devices, a new metric, termed correlation-aware AoI, has been developed and optimized for unmanned aerial vehicle (UAV) networks in [9]. Recently, the application of advanced physical layer communication techniques, such as hybrid automatic repeat request (H-ARQ) and cooperative communications, to improve the AoI of wireless networks with one source-destination pair has been considered in [10] and [11], respectively.

For the scenario with multiple users, the AoI analysis is more challenging than that for the single-user scenario. This is due to the fact that multiple users are competing in the same transmission medium, i.e., one user's update might be preempted by another's and hence its AoI is affected by the other users' transmission strategies. The AoI realized by wireless transmission with various random access protocols has been characterized in [12]–[14]. We note that in many wireless networks, the potential collision between multiple users is avoided by applying orthogonal multiple access (OMA) techniques, such as frequency division multiple access (FDMA) and time division multiple access (TDMA). In [15], the impact of these OMA techniques on the AoI has been studied, where TDMA was shown to outperform FDMA in terms of the averaged AoI. As non-orthogonal multiple access (NOMA) is more spectrally efficient than OMA, it is natural to consider the use of NOMA for improving the AoI of wireless networks [16]. The authors of [17] focused on a two-user scenario and showed that the spectral efficiency gain of NOMA over OMA indeed can be transferred to a reduction of the AoI. In order to minimize the AoI, a dynamic policy to switch between NOMA and OMA was developed by formulating the AoI minimization problem as a Markov decision process problem. In [18], the impact of stochastic arrivals on the AoI achieved by NOMA was studied, where the performance gain of NOMA over OMA was shown to be significant for large arrival rates. In [19], the AoI of NOMA assisted grant-free transmission was minimized by applying the tool of evolutionary game. In [20], the AoI realized by reconfigurable intelligent surface (RIS) assisted NOMA transmission was analyzed, and the application of NOMA to reduce the AoI of satellite communications was considered in [21].

This paper considers a general multi-user uplink communication network, where OMA has

already been deployed to serve the multiple users, i.e., there is a legacy network based on OMA. Because TDMA outperforms FDMA in terms of AoI, TDMA is considered as an example for OMA in this paper. Unlike the schemes reported in [22] and [23], which require a change of the time frame structure of the legacy TDMA network, in this paper, NOMA is applied as an add-on to the TDMA legacy network. This means that the AoI is reduced with minimal disruption to the legacy network, and hence the proposed NOMA protocols can be practically implemented in various existing communication systems which are based on OMA. The main contributions of the paper are the characterization of the AoI achieved by the proposed NOMA protocols and also the identification of the benefits of using NOMA to reduce the AoI of wireless networks, as explained in the following:

- For the case where each user's update is generated at the beginning of its transmit time slot, cognitive-radio inspired NOMA (CR-NOMA) is applied to ensure that each user has two opportunities to deliver its update to the base station in each TDMA time frame [24]. A closed-form expression for the AoI realized by CR-NOMA is developed to facilitate the performance evaluation, and an asymptotic analysis reveals that at high signal-to-noise ratio (SNR), CR-NOMA and TDMA realize the same AoI. This conclusion is expected since, at high SNR, each user needs one transmission only to ensure that its update is successfully delivered to the base station. However, at low SNR, the use of CR-NOMA can result in significant AoI reduction compared to TDMA, which demonstrates that one benefit of using NOMA is to offer users more chances to transmit, i.e., by using NOMA the users can update their base station more frequently.
- For the case where each user's update is generated at the beginning of a TDMA time frame, a modified CR-NOMA protocol is developed to demonstrate another benefit of using NOMA to improve the AoI. In particular, the modified CR-NOMA protocol effectively reduces the users' access delay, i.e., the users are scheduled to transmit earlier than in the TDMA case, which is useful for improving the freshness of the data available at the base station. For example, a user which is scheduled in a time slot close to the end of a TDMA frame experiences severe access delay and hence suffers from a large AoI with TDMA, because it has to wait for a long time before it can send its update which has been generated at the beginning of the frame. The use of NOMA ensures that this user can jump the queue and transmit earlier than with TDMA. An exact expression for the AoI achieved with the

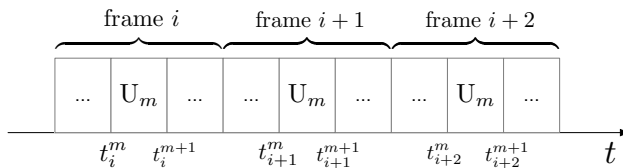


Fig. 1. Considered TDMA time frame structure.

modified CR-NOMA protocol is obtained, and an asymptotic analysis demonstrates that the use of NOMA yields a reduction of AoI at high SNR, compared to TDMA.

The remainder of this paper is organized as follows. In Section II, the system model and the considered data generation models are described. In Sections III and IV, two CR-NOMA based transmission protocols are introduced and their impact on the AoI is characterized. Simulation results are presented in Section IV, and the paper is concluded in Section V. Finally, all the proofs are collected in the appendix.

II. SYSTEM MODEL

Consider a communication network with M users, denoted by U_m , $1 \leq m \leq M$, sending their updates to the same base station. Assume that an OMA based legacy network has been employed to serve these users. Because TDMA yields smaller AoI than FDMA [15], TDMA is used as an example of OMA in this paper. There are M time slots in each TDMA time frame and U_m is scheduled to transmit in the m -th time slot of each frame with transmit power P , as shown in Fig. 1. Denote the duration of each time slot by T s, and the start of the m -th time slot in the i -th frame by t_i^m , $1 \leq m \leq M$. Therefore, with TDMA, each user can deliver one update to the base station every MT s.

A. AoI Model

AoI indicates the freshness of the updates successfully delivered to the base station and can be defined as follows. At time t , denote by $T_m(t)$ the generation time of the freshest update successfully delivered from U_m to the base station. Therefore, U_m 's instantaneous AoI is defined as follows [1]:

$$\Delta_m(t) = t - T_m(t). \quad (1)$$

The normalized overall average AoI of the considered network is given by

$$\bar{\Delta} = \frac{1}{M} \sum_{m=1}^M \underbrace{\lim_{T \rightarrow \infty} \frac{1}{T} \int_0^T \Delta_m(t) dt}_{\Delta_m}. \quad (2)$$

B. Data Generation Models

When data is generated has significant impact on the AoI, and the following two types of data generation are considered in this paper:

1) *The generate-at-will (GAW) model:* This model assumes that a new update is generated right before the transmit time slot of the user [1], [17], [22]. For example, if a user decides to transmit in the m -th time slot of the i -th frame, the update to be sent in this time slot is generated at t_i^m , as shown in Fig. 2(a). As a widely used data generation model, GAW has the advantage of improving the freshness of the data by always transmitting a freshly generated update. However, GAW potentially results in high system complexity as a user is required to repeatedly generate updates if the user is offered multiple chances to transmit in a short period.

2) *The generate-at-request (GAR) model:* With this model, the base station requests each user to generate an update at the beginning of each time frame, instead of each time slot, as shown in Fig. 2(b). If retransmission is carried out within one frame, the same update will be sent. GAR is crucial to synchronized sensing, and hence important in many Internet of Things (IoT) applications, such as structural health monitoring and autonomous driving [25], [26]. GAR can lead to larger AoI than GAW, since a user's access delay, i.e., the duration between the generation time of an update and the corresponding transmit time, is included in the calculation of AoI. However, compared to GAW, GAR can reduce system complexity and energy consumption, since GAR avoids asking the users to repeatedly generate updates for retransmission.

C. CR-NOMA Transmission

CR-NOMA can be used as an add-on to TDMA to improve the freshness of the data collected in the network, as explained in the following. To reduce system complexity, the following simple user pairing scheme is considered. In particular, U_m and $U_{m'}$, where $1 \leq m \leq \frac{M}{2}$ and $m' = m + \frac{M}{2}$, are paired together to share the spectrum, and are allowed to transmit simultaneously in the m -th and the m' -th time slots of each frame ¹.

¹For illustrative purposes, it is assumed that M is an even number, but the proposed protocol can be straightforwardly extended to the case with an odd number of users, e.g., one of the users can be simply served by TDMA.

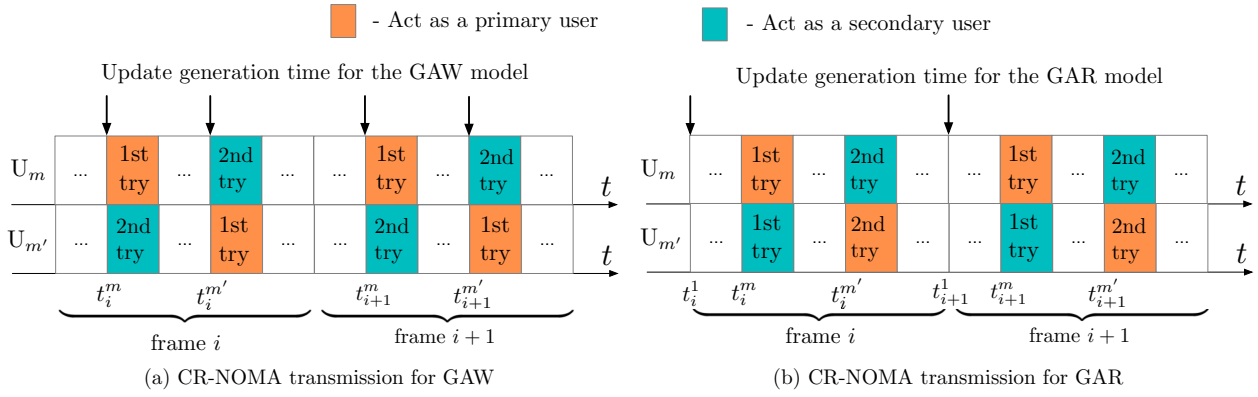


Fig. 2. Illustration for the two proposed CR-NOMA transmission schemes.

The aim of CR-NOMA transmission is to increase the likelihood for each user to deliver one update to the base station every MT s, compared to TDMA. Depending on the used data generation model, the application of CR-NOMA transmission is slightly different. In brief, for GAW, U_m and $U_{m'}$ use the m -th and the m' -th time slots of each frame for their first tries for updating, respectively, as shown in Fig. 2(a). If their first tries are not successful, U_m uses the m' -th time slot of the current frame, and $U_{m'}$ uses the m -th time slot of the next frame for retransmission. For GAR, both the users use the m -th time slot for their first tries and the m' -th time slot for their second tries, as shown in Fig. 2(b). The details of CR-NOMA transmission are provided as follows.

1) *CR-NOMA Transmission for GAW*: In the m -th time slot of the i -th frame, U_m is treated as the primary user and is scheduled to transmit with transmit power P , in the same manner as TDMA. If this transmission is not successful, U_m is offered another chance to transmit in the m' -th time slot as the secondary user with transmit power P^S , where $U_{m'}$ is treated as the primary user in this time slot. To ensure that the implementation of NOMA is transparent to the primary user, the secondary user's signal is decoded in the first stage of successive interference cancellation (SIC) at the base station and its data rate needs to be capped [24]. For example, in the m' -th time slot, U_m is the secondary user and its data rate, denoted by $R_{m,i}^S$, is capped as follows:

$$R_{m,i}^S \leq \log \left(1 + \frac{P^S |h_m^{i,m'}|^2}{P |h_{m'}^{i,m'}|^2 + 1} \right), \quad (3)$$

where the binary logarithm is used, and U_n 's channel gain in the k -th time slot of the i -th frame is denoted by $h_n^{i,k}$. We note that the noise power is assumed to be normalized, and hence P and P^S are the effective transmit SNRs. The users' channel gains in different time slots are

assumed to be independent and identically distributed (i.i.d.) and follow the complex Gaussian distribution with zero mean and unit variance.

Similarly, in the m' -th time slot of the i -th frame, $U_{m'}$ is scheduled to transmit as the primary user, in the same manner as in TDMA. If this transmission is not successful, the user will use the m -th time slot of the next frame to transmit a new update. Because $U_{m'}$ is the secondary user in the m -th time slot, its data rate in this time slot needs to be capped similarly as in (3).

2) *CR-NOMA Transmission for GAR*: Recall that with GAR, the users' updates are generated at the beginning of each TDMA frame. On the one hand, in order to reduce the access delay, $U_{m'}$ will not wait for the m' -th time slot, but use the m -th time slot to deliver its update. We note that U_m is treated as the primary user in the m -th time slot, which means that $U_{m'}$'s data rate needs to be capped similarly as in (3). Only if $U_{m'}$'s transmission in the m -th time slot is not successful, $U_{m'}$ carries out a retransmission in the m' -th time slot of the current frame.

On the other hand, U_m 's transmission strategy for GAR in the m -th time slot is the same as that for GAW. If U_m requires a retransmission, it will be treated as the secondary user in the m' -th time slot, and its achievable data rate in this time slot depends on its partner's transmission strategy, which is different from that for GAW. In particular, if $U_{m'}$'s transmission in the m -th time slot is not successful, a retransmission from $U_{m'}$ in the m' -th time slot is needed, and hence U_m 's data rate in this time slot is capped as in (3). However, if $U_{m'}$'s transmission in the m -th time slot is successful, $U_{m'}$ keeps silent in the m' -th time slot, which means that U_m 's achievable data rate in this time slot is simply given by:

$$R_{m,i}^S = \log \left(1 + P^S |h_m^{i,m'}|^2 \right). \quad (4)$$

The AoI achieved by CR-NOMA transmission for the two data generation models will be analyzed in the following two sections, respectively.

III. AOI OF CR-NOMA TRANSMISSION FOR GAW

In this section, the AoI achieved by CR-NOMA is studied the GAW model, where TDMA is used as a benchmarking scheme. The benefit of using CR-NOMA to reduce the AoI can be clearly illustrated with the example shown in Fig. 3. Because GAW is used, the instantaneous AoI is reduced to T whenever an update is successfully delivered to the base station. For the illustrated example, U_m fails to deliver its update to the base station in the m -th time slot of the $(i + 1)$ frame. With TDMA, the user has to wait until the next TDMA frame. However, with

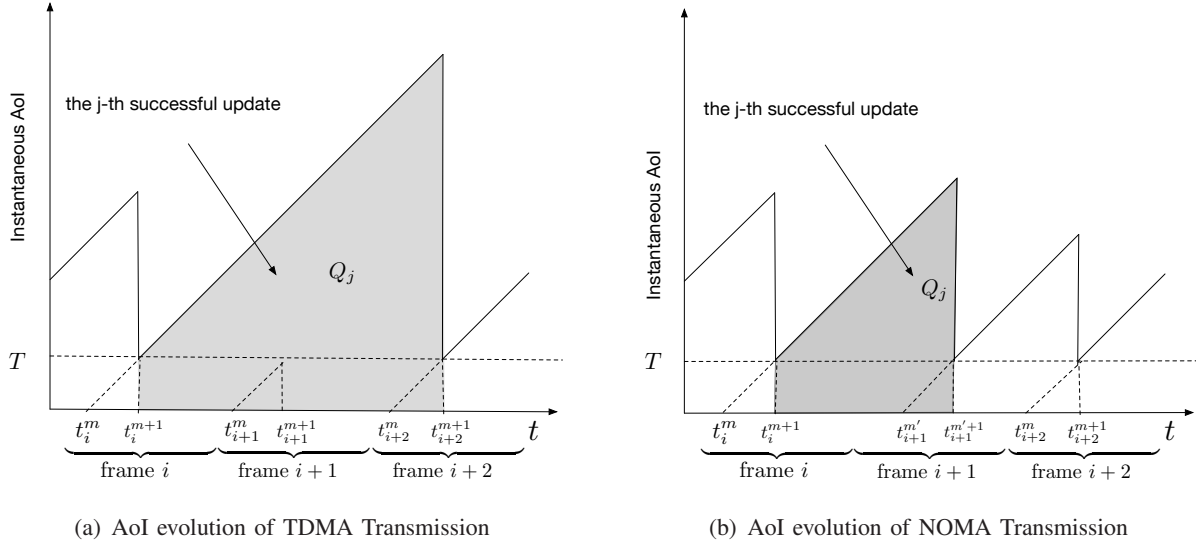


Fig. 3. Illustration of AoI evolution for the two considered transmission protocols. The generate-at-will model is considered. For TDMA, U_m relies on the m -th time slot of each frame, i.e., from t_i^m to t_{i+1}^{m+1} in frame i . For the illustrated example, U_m successfully delivers its update in frames i and $(i+2)$, but fails in frame $(i+1)$. For NOMA, the user also fails in the m -th time slot of frame $(i+1)$, but successfully delivers its update in the m' -th ($m' = m + \frac{M}{2}$) time slot of the same frame, which improves data freshness.

NOMA, the user has another chance for retransmission in the current frame, which is helpful to reduce the AoI.

A. AoI Realized for TDMA

The AoI realized for TDMA can be straightforwardly analyzed as follows. Without loss generality, we focus on U_m 's average AoI realized for TDMA, denoted by $\bar{\Delta}_m^T$. Further denote the number of frames between the $(j-1)$ -th and the j -th successful updates by x_j . In Fig. 3(a), an example with $x_j = 2$ is shown. Therefore, finding the average AoI for TDMA is equivalent to find the area of the shaded region in Fig. 3(a), denoted by Q_j , which means that $\bar{\Delta}_m^T$ can be expressed as follows:

$$\bar{\Delta}_m^T = \lim_{J \rightarrow \infty} \frac{\sum_{j=1}^J Q_j}{\sum_{j=1}^J x_j MT} = T + \frac{MT}{2} \frac{\mathcal{E}\{X^2\}}{\mathcal{E}\{X\}}, \quad (5)$$

where J denotes the total number of the successful updates, $Q_j = x_j MT^2 + \frac{1}{2} x_j^2 M^2 T^2$, $\mathcal{E}\{X\} = \lim_{J \rightarrow \infty} \frac{1}{J} \sum_{j=1}^J x_j$, and $\mathcal{E}\{X^2\} = \lim_{J \rightarrow \infty} \frac{1}{J} \sum_{j=1}^J x_j^2$. Since the users' channel gains are assumed to be i.i.d., x_j follows the geometric distribution, i.e., the probability mass function of x_j is given by $\mathbb{P}(X = x_j) = p_e^{x_j-1} (1 - p_e)$, where p_e denotes the probability for the event that a user fails to deliver an update in a time slot with T s. By using the assumptions that each update contains N

bits and the users' channel gains are complex Gaussian distributed, $p_e = \mathbb{P}(T \log(1 + P|h_m^{i,m'}|^2) \leq N) = 1 - e^{-\frac{\epsilon}{P}}$, where $\epsilon = 2^{\frac{N}{T}} - 1$. As a result, the normalized average AoI achieved by TDMA can be obtained as follows:

$$\bar{\Delta}^T \stackrel{(1)}{=} \bar{\Delta}_m^T \stackrel{(2)}{=} T + \frac{MT}{2} (2e^{\frac{\epsilon}{P}} - 1), \quad (6)$$

where the first step follows by the fact that the users experience the same AoI in TDMA, and the second step follows by using the mean and the variance of the geometric distribution.

B. AoI Realized for CR-NOMA

The analysis of the AoI realized with CR-NOMA is more challenging than that for TDMA. The reason is that each user has two transmission opportunities in each TDMA frame, which means that the time interval between the two adjacent successful updates is not always a multiple of MT . The following lemma provides a closed-form expression for the AoI realized by CR-NOMA.

Lemma 1. *For the case of the GAW model, the normalized overall average AoI realized by CR-NOMA is given by*

$$\bar{\Delta}^N = T + \Delta(p_0, p_m, p_{m'}), \quad (7)$$

where $\Delta(x, y, z)$ is defined as follows:

$$\Delta(x, y, z) = \frac{MT}{4} \frac{2(y+z)^2(1+x) + yz(1-x)^2}{(y+z)^2(1-x)}, \quad (8)$$

$$p_m = e^{-\frac{\epsilon}{P^S}}, \quad p_{m'} = \left(1 - e^{-\frac{\epsilon}{P^S}}\right) e^{-\frac{\epsilon}{P^S}} \frac{1}{1 + \frac{P\epsilon}{P^S}}, \quad \text{and} \quad p_0 = \left(1 - e^{-\frac{\epsilon}{P^S}}\right) \left(1 - \frac{e^{-\frac{\epsilon}{P^S}}}{1 + \frac{P\epsilon}{P^S}}\right).$$

Proof. See Appendix A. □

Based on the closed-form expression of the AoI given in Lemma 1, an asymptotic analysis can be carried out to obtain an insightful understanding of the impact of NOMA on the AoI. For example, consider the following high SNR scenario, $P^S = P \rightarrow \infty$, which means that $p_m \approx 1 - \frac{\epsilon}{P}$. $p_{m'}$ can be approximated as follows:

$$p_{m'} = \left(1 - e^{-\frac{\epsilon}{P^S}}\right) e^{-\frac{\epsilon}{P^S}} \frac{1}{1 + \frac{P\epsilon}{P^S}} \approx \frac{\epsilon}{P(1 + \epsilon)}. \quad (9)$$

Furthermore, p_0 can be approximated at high SNR as follows:

$$p_0 = \left(1 - e^{-\frac{\epsilon}{P^S}}\right) \left(1 - \frac{e^{-\frac{\epsilon}{P^S}}}{1 + \frac{P\epsilon}{P^S}}\right) \approx \frac{\epsilon^2}{P(1 + \epsilon)}.$$

By using the high-SNR approximations of p_0 , p_m and $p_{m'}$, the AoI achieved by CR-NOMA can be approximated as follows:

$$\begin{aligned}\bar{\Delta}^N &\approx T + \frac{MT}{4} \frac{2(p_m + p_{m'})^2 + p_m p_{m'}}{(p_m + p_{m'})^2} \\ &\stackrel{(1)}{\approx} T + \frac{MT}{4} \frac{2(p_m)^2}{(p_m)^2} = T + \frac{MT}{2},\end{aligned}\quad (10)$$

where step 1 follows by the fact that $p_m \gg p_{m'}$ at high SNR.

On the other hand, the AoI realized by TDMA can be approximated at high SNR as follows:

$$\bar{\Delta}^T = T + \frac{MT}{2}(2e^{\frac{\epsilon}{P}} - 1) \approx T + \frac{MT}{2}.\quad (11)$$

Comparing the AoI shown in (10) and (11), the following corollary can be obtained.

Corollary 1. *For the case of the GAW model, at high SNR, i.e., $P = P^S \rightarrow \infty$, the normalized average AoI achieved by CR-NOMA is same as that of TDMA .*

Remark 1: The conclusion shown in Corollary 1 is expected since, at high SNR, U_m 's first try, i.e., its transmission in the m -th time slot, is almost guaranteed to be successful. Therefore, retransmission is not needed at high SNR, and CR-NOMA is reduced to TDMA, which explains why the two protocols achieve the same AoI at high SNR. However, it is important to point out that the use of CR-NOMA can result in a significant performance gain over TDMA in the low SNR regime, as shown in the simulation section.

Remark 2: The use of CR-NOMA means that a user may need to transmit two times every MT s, which can cause a higher energy consumption than for TDMA. In order to avoid this drawback, prior to its transmit time slot, a user can first calculate its data rate supported by CR-NOMA, and transmit only if this data rate is sufficient to deliver its update. This implementation requires that each user knows its own channel state information (CSI) as well as that of its partner. This CSI assumption can be realized as follows. The base station first broadcasts a pilot signal before a time slot, and then each user carries out channel estimation individually. In addition, the CSI of each user's partner can be obtain either via device-to-device communication between the partners or via a dedicated control channel.

IV. AOI OF CR-NOMA TRANSMISSION FOR GAR

Unlike the GAW model, the GAR model requires the users to generate their updates at the beginning of each frame, which means that the access delay needs to be included in the AoI.

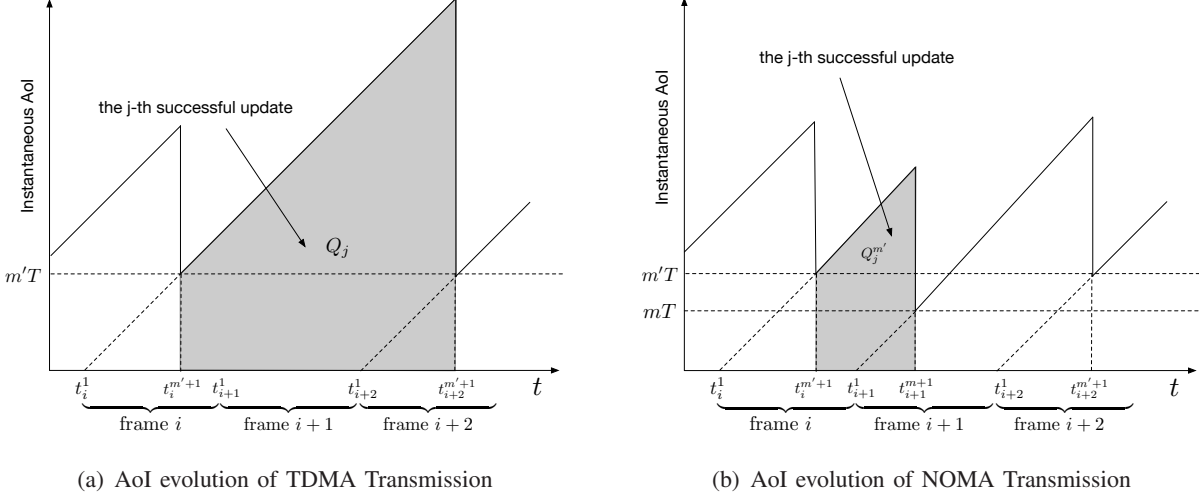


Fig. 4. Illustration of AoI evolution for the considered protocols. The generate-at-request model is considered. For the illustrated example, $U_{m'}$ successfully delivers its update in frames i and $(i + 2)$, but fails in the m' -th time slot of frame $(i + 1)$ for TDMA. For NOMA, the user successfully delivers its update by using the m -th time slot of frame $(i + 1)$, which improves data freshness.

The impact of the access delay on the AoI can be illustrated by using Fig. 4, where $U_{m'}$'s AoI experience is considered. With TDMA, $U_{m'}$ has to wait until the m' -th time slot of each frame for its transmission. This means that the user's instantaneous AoI drops to $m'T$, since its update is generated at the beginning of the frame. With CR-NOMA, $U_{m'}$ can also use the m -th time slot of each frame, which results in two benefits for reducing the AoI. One is that with two chances to transmit every MT s, the likelihood of a failed update is reduced, which is similar to the GAR case. The second benefit is that the use of NOMA can effectively reduce the access delay, since $U_{m'}$ can transmit earlier than for TDMA by using the m -th time slot instead of the m' -th time slot, and its instantaneous AoI can drop to mT .

A. AoI Realized for TDMA

To be consistent with the illustration of Fig. 4, $U_{m'}$'s AoI is considered, but U_m 's AoI can be analyzed similarly. As shown in Fig. 4(a), in TDMA, $U_{m'}$ is allowed to use the m' -th time slot only, i.e., its transmit time slot ends at $t_i^{m'+1}$ in the i -th frame, where it is important to point out that its update is generated at t_i^1 . Again denote by x_j the number of frames between the $(j - 1)$ -th and the j -th successful updates, where an example with $x_j = 2$ is shown in Fig. 4.

Similar to the GAW case, the time span between the two adjacent successful updates is $x_j MT$; however, the AoI does not drop to T whenever there is a successful update. Instead, the AoI drops to $m'T$ only, because $U_{m'}$'s update is generated at the beginning of the frame. Therefore,

$U_{m'}$'s averaged AoI achieved by TDMA is given by

$$\begin{aligned}\bar{\Delta}_{m'}^T &= \lim_{J \rightarrow \infty} \frac{\sum_{j=1}^J Q_j}{\sum_{j=1}^J x_j MT} \\ &= \lim_{J \rightarrow \infty} \frac{\sum_{j=1}^J (m'T x_j MT + \frac{1}{2} x_j^2 M^2 T^2)}{\sum_{j=1}^J x_j MT} = m'T + \frac{MT \mathcal{E}\{x_j^2\}}{2 \mathcal{E}\{x_j\}}.\end{aligned}\quad (12)$$

By using steps similar to those in Section III-A, $U_{m'}$'s averaged AoI achieved by TDMA for the GAR model can be obtained as follows:

$$\bar{\Delta}_{m'}^T = m'T + \frac{MT}{2} (2e^{\frac{\epsilon}{P}} - 1). \quad (13)$$

Comparing (5) to (13), one can find that with the GAR model, the users experience a larger AoI, which is mainly due to the access delay, i.e., a user generates its update at the beginning of one frame but has to wait for its turn to deliver the update.

B. AoI Realized for CR-NOMA

The AoI realized by CR-NOMA in the GAR case is challenging to analyze due to the fact that a user's instantaneous AoI does not always drop to the same value, which is different from the GAW case. In particular, in the GAW case, a user's instantaneous AoI is always reduced to T , regardless which time slot is used for update delivery. However, in the GAR case, if U_m successfully delivers its update in the m -th time slot of a frame, its instantaneous AoI drops to mT , whereas its instantaneous AoI drops to $m'T$ if the transmission in the m' -th time slot is successful. What makes the AoI analysis more complicated is that the calculation of the shaded region $Q_j^{m'}$ shown in Fig. 4 does not only depend on which time slot is used for the $(j-1)$ -th successful update but also on which time slot is used for the j -th successful update. Furthermore, whether a user can successfully deliver its update to the base station is also affected by its partner's transmission strategy, as discussed in Section II-C. The following lemma provides a closed-form expression for the AoI realized by CR-NOMA in the GAR case.

Lemma 2. *For the case of the GAR model, U_k 's average AoI realized by CR-NOMA is given by*

$$\bar{\Delta}_k^N = \Delta_{k,0} + \Delta(p_{0k}, p_{mk}, p_{m'k}), \quad (14)$$

where $k \in \{m, m'\}$, $1 \leq m \leq \frac{M}{2}$, $\Delta_{k,0}$ is given by

$$\Delta_{k,0} = \frac{(1 - p_{0k})^2}{(p_{mk} + p_{m'k})^2} \left[\left((p_{mk} + p_{m'k}) \frac{mT p_{mk}}{(1 - p_{0k})^2} + \frac{p_{m'k}}{2} \frac{mT p_{mk}}{1 - p_{0k}} \right) \right. \quad (15)$$

$$\left. + \left((p_{mk} + p_{m'k}) \frac{m'T p_{m'k}}{(1 - p_{0k})^2} - \frac{p_{mk}}{2} \frac{m'T p_{m'k}}{1 - p_{0k}} \right) \right], \quad (16)$$

$p_{mm} = e^{-\frac{\epsilon}{P^S}}$, $p_{m'm} = \left(1 - e^{-\frac{\epsilon}{P}} - e^{-\frac{\epsilon}{P^S}} \tau\right) e^{-\frac{\epsilon}{P^S}} \frac{1}{1 + \frac{P\epsilon}{P^S}} + e^{-\frac{2\epsilon}{P^S}} \tau$, $p_{0m} = \left(1 - e^{-\frac{\epsilon}{P}} - e^{-\frac{\epsilon}{P^S}} \tau\right) \left(1 - \frac{\frac{\epsilon}{P^S}}{1 + \frac{P\epsilon}{P^S}}\right) + e^{-\frac{\epsilon}{P^S}} \tau \left(1 - e^{-\frac{\epsilon}{P^S}}\right)$, $p_{0m'} = \left(1 - e^{-\frac{\epsilon}{P^S}} \frac{1}{1 + \frac{P\epsilon}{P^S}}\right) \left(1 - e^{-\frac{\epsilon}{P}}\right)$, $p_{mm'} = e^{-\frac{\epsilon}{P^S}} \frac{1}{1 + \frac{P\epsilon}{P^S}}$, $p_{m'm'} = \left(1 - e^{-\frac{\epsilon}{P^S}} \frac{1}{1 + \frac{P\epsilon}{P^S}}\right) e^{-\frac{\epsilon}{P}}$ and $\tau = \frac{1 - e^{-\left(\frac{\epsilon}{P^S} P + 1\right) \frac{\epsilon}{P}}}{\frac{\epsilon}{P^S} P + 1}$. The normalized overall average AoI realized by CR-NOMA is given by $\bar{\Delta}^N = \frac{1}{M} \sum_{m=1}^{\frac{M}{2}} (\bar{\Delta}_m^N + \bar{\Delta}_{m'}^N)$.

Proof. See Appendix B. □

Although the AoI expression shown in Lemma 2 is lengthy and complicated, it can be used to obtain an insightful understanding of the impact of NOMA on the AoI. Let us consider the high SNR scenario, i.e., $P^S = P \rightarrow \infty$. Because the use of NOMA reduces the access delay for $U_{m'}$, it is expected that $U_{m'}$'s AoI experience for TDMA and NOMA will be significantly different, and hence we focus on $U_{m'}$'s AoI in the following.

With some straightforward algebraic manipulations, at high SNR, the following approximations can be obtained: $p_{0m'} \approx \frac{\epsilon}{1 + \epsilon} \frac{\epsilon}{P}$, $p_{mm'} \approx \frac{1 - \frac{\epsilon}{P}}{1 + \epsilon}$, and $p_{m'm'} \approx \frac{\epsilon}{1 + \epsilon} \left(1 - \frac{\epsilon}{P}\right)$, which lead to the following approximation: $p_{mm'} + p_{m'm'} \approx 1 - \frac{\epsilon}{P}$. On the one hand, by using these approximations, the first term in (14), $\Delta_{m',0}$, can be approximated at high SNR as follows:

$$\begin{aligned} \Delta_{m',0} &\approx \frac{1}{\left(1 - \frac{\epsilon}{P}\right)^2} \left[\left(\left(1 - \frac{\epsilon}{P}\right) mT \frac{1 - \frac{\epsilon}{P}}{1 + \epsilon} + \frac{\epsilon \left(1 - \frac{\epsilon}{P}\right)}{2(1 + \epsilon)} mT \frac{1 - \frac{\epsilon}{P}}{1 + \epsilon} \right) \right. \quad (17) \\ &\quad \left. + \left(\left(1 - \frac{\epsilon}{P}\right) m'T \frac{\epsilon \left(1 - \frac{\epsilon}{P}\right)}{1 + \epsilon} - \frac{1 - \frac{\epsilon}{P}}{2(1 + \epsilon)} m'T \frac{\epsilon \left(1 - \frac{\epsilon}{P}\right)}{1 + \epsilon} \right) \right] \\ &= \frac{1}{(1 + \epsilon)^2} \left[mT(1 + \epsilon) + \frac{\epsilon}{2} mT + m'T \epsilon (1 + \epsilon) - \frac{1}{2} m'T \epsilon \right]. \end{aligned}$$

On the other hand, the second term in (14), $\Delta(p_{0m'}, p_{mm'}, p_{m'm'})$, can be approximated as follows:

$$\begin{aligned} \Delta(p_{0m'}, p_{mm'}, p_{m'm'}) &= \frac{MT}{4} \frac{2(p_{mm'} + p_{m'm'})^2 (1 + p_{0m'}) + p_{mm'} p_{m'm'} (1 - p_{0m'})^2}{(p_{mm'} + p_{m'm'})^2 (1 - p_{0m'})} \quad (18) \\ &\approx \frac{MT}{4} \frac{2 \left(1 - \frac{\epsilon}{P}\right)^2 + \frac{1 - \frac{\epsilon}{P}}{1 + \epsilon} \frac{\epsilon}{1 + \epsilon} \left(1 - \frac{\epsilon}{P}\right)}{\left(1 - \frac{\epsilon}{P}\right)^2} \\ &\approx \frac{MT}{2} \left(1 + \frac{\epsilon}{2(1 + \epsilon)^2}\right). \end{aligned}$$

Therefore, $U_{m'}$'s AoI can be approximated at high SNR as follows:

$$\begin{aligned}\bar{\Delta}_{m'}^N &= \Delta_{m',0} + \Delta(p_{0m'}, p_{mm'}, p_{m'm'}) \\ &\approx \frac{1}{(1+\epsilon)^2} \left[mT(1+\epsilon) + \frac{\epsilon}{2}mT + m'T\epsilon(1+\epsilon) - \frac{1}{2}m'T\epsilon \right] + \frac{1}{2}MT \left(1 + \frac{\epsilon}{2(1+\epsilon)^2} \right) \\ &= \frac{1}{(1+\epsilon)} [mT + m'T\epsilon] + \frac{1}{2}MT,\end{aligned}\tag{19}$$

where the last step follows by using the fact that $m' = m + \frac{M}{2}$.

Recall that $U_{m'}$'s AoI for TDMA can be approximated at high SNR as follows: $m'T + \frac{MT}{2}$. Therefore, the difference between $U_{m'}$'s AoI for TDMA and NOMA, denoted by $D_{m'}$, is given by

$$\begin{aligned}D_{m'} &\triangleq \frac{1}{(1+\epsilon)} [mT + m'T\epsilon] + \frac{1}{2}MT - \left(m'T + \frac{MT}{2} \right) \\ &= \frac{1}{(1+\epsilon)} [mT + m'T\epsilon] - m'T \\ &= \frac{mT + m'T\epsilon - m'T - m'T\epsilon}{(1+\epsilon)} = -\frac{MT}{2(1+\epsilon)} < 0,\end{aligned}\tag{20}$$

which means that $U_{m'}$ experiences less AoI for NOMA than for TDMA.

In order to find a high-SNR approximation for $\bar{\Delta}_m^N$, the following approximations can be obtained first: $\tau \approx \frac{\epsilon}{P}$, $p_{mm} \approx 1 - \frac{\epsilon}{P}$, $p_{m'm} \approx \frac{\epsilon}{P} \frac{1-\epsilon}{1+\epsilon} + \frac{\epsilon}{P}$, and $p_{0m} \approx \frac{\epsilon}{P} \frac{\epsilon}{1+\epsilon}$. By applying these approximations and also using steps similar to those used for approximating $\bar{\Delta}_{m'}^N$, U_m 's AoI can be approximated at high SNR as follows:

$$\bar{\Delta}_m^N = \Delta_{m,0} + \Delta(p_{0m}, p_{mm}, p_{m'm}) \approx mT + \frac{MT}{2},\tag{21}$$

which is identical to the case of TDMA. Therefore, the following corollary can be obtained.

Corollary 2. *For the case with the GAR model, at high SNR, i.e., $P = P^S \rightarrow \infty$, $U_{m'}$'s average AoI for CR-NOMA is strictly smaller than that for TDMA. U_m 's average AoIs for TDMA and CR-NOMA are identical at high SNR.*

Remark 3: For $U_{m'}$, the performance gain of NOMA over TDMA at high SNR is due to the fact that the use of NOMA reduces the access delay, which is particularly important in the GAR case. Recall that in the GAR case, a user's update is generated at the beginning of the TDMA frame, which means that a user which is scheduled later in the frame suffers from a larger AoI. The use of NOMA always ensures that $U_{m'}$ does not have to wait until the m' -th time slot,

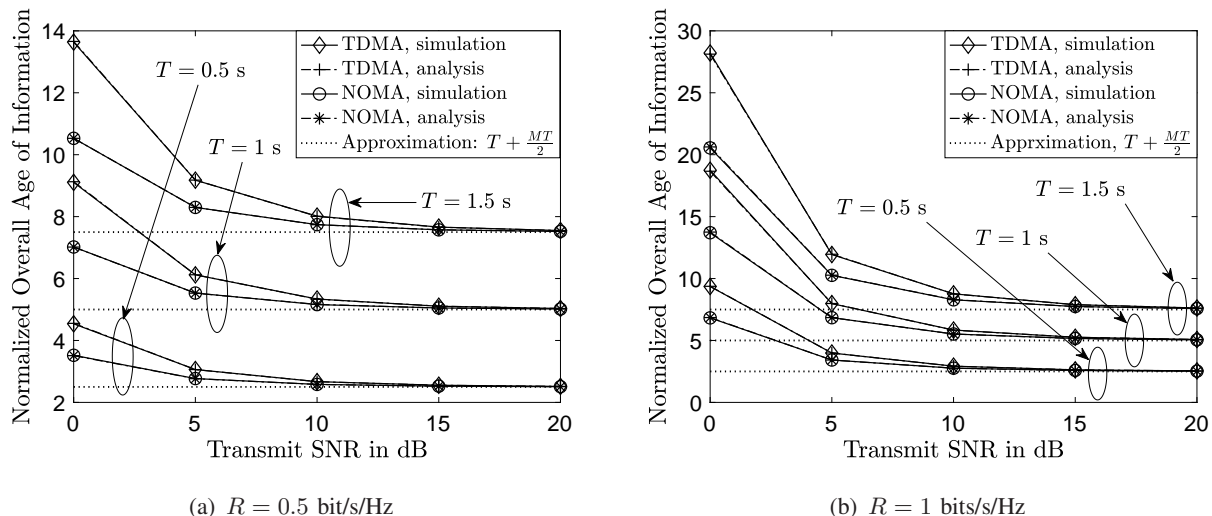


Fig. 5. The impact of NOMA transmission on the AoI for the generate-at-will model with $M = 8$.

but can transmit earlier, i.e., in the m -th time slot, which leads to the AoI reduction stated in Corollary 2. We note that the use of NOMA does not improve U_m 's access delay, which is the reason why U_m 's AoIs for TDMA and NOMA are identical at high SNR.

Remark 4: We further note that the AoI reduction due to the use of CR-NOMA is important to improve user fairness. For example, two user which are scheduled in the first and the last time slots of a frame experience significantly different AoI for TDMA, but the use of CR-NOMA can reduce the difference between the users' AoI experience.

V. NUMERICAL STUDIES

In this section, the benefits of NOMA transmission regarding the AoI are studied by using computer simulation results, where TDMA is used as a benchmarking scheme. The time frame structure shown in Fig. 1 is used, where the users' channel gains in different time slots are assumed to be i.i.d. complex Gaussian distributed with zero mean and unit variance. For illustration, define $R \triangleq \frac{N}{T}$ and assume that $P = P^S$, where P is termed the transmit SNR in the simulation section because the noise power is assumed to be normalized. Because the AoI depends on the data generation models, the benefits of NOMA for AoI reduction are studied in two different subsections in the following.

A. The Generate-at-Will Model

Recall that for the GAW model, each user generates a new update at the beginning of its transmit time slot. The impact of the different transmission protocols on the AoI is investigated

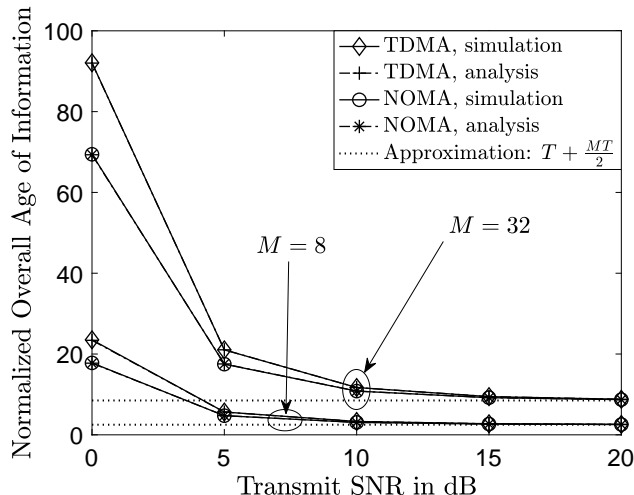


Fig. 6. The impact of the number of users, M , on the AoI, for the generate-at-will model with $R = 1.5$ bits/s/Hz and $T = 0.5$ s.

in Fig. 5 by assuming that there are $M = 8$ users, i.e., there are 8 time slots in each TDMA frame. As can be seen from the two subfigures in Fig. 5, the AoI achieved by the proposed NOMA transmission protocol can be significantly lower than that for TDMA. For example, for $R = 1$ bits/s/Hz, $T = 1.5$ s, and a transmit SNR of 0 dB, the AoI realized with TDMA is around 28, and the AoI achieved by CR-NOMA is just 20, which means that the use of CR-NOMA yields more than a one-quarter reduction compared to TDMA. However, at high SNR, Fig. 5 shows that TDMA and NOMA yield the same AoI, which confirms Corollary 1. We also note that both subfigures in Fig. 5 verify the accuracy of the analytical results presented in Lemma 1 as well as the approximation result developed in (10).

Fig. 5 also shows the impact of R on the AoI performance of the considered transmission protocols. In particular, by comparing Fig. 5(a) and Fig. 5(b), one can observe that increasing R increases the AoI for both transmission protocols. Recall that increasing R for given value of T means that there are more bits contained in each update, which makes transmission failures more likely and hence increases the AoI. We note that the performance gain of NOMA over TDMA becomes larger for larger R . For example, for $T = 1.5$ s and a transmit SNR of 0 dB, the performance gain of NOMA over TDMA if $R = 0.5$ bits/s/Hz is 3, and this performance gain can be increased to almost 8 if $R = 1$ bits/s/Hz. The subfigures in Fig. 5 also show that the AoI realized by the considered protocols increases with T , since increasing T for given R means that there are more bits contained in each update.

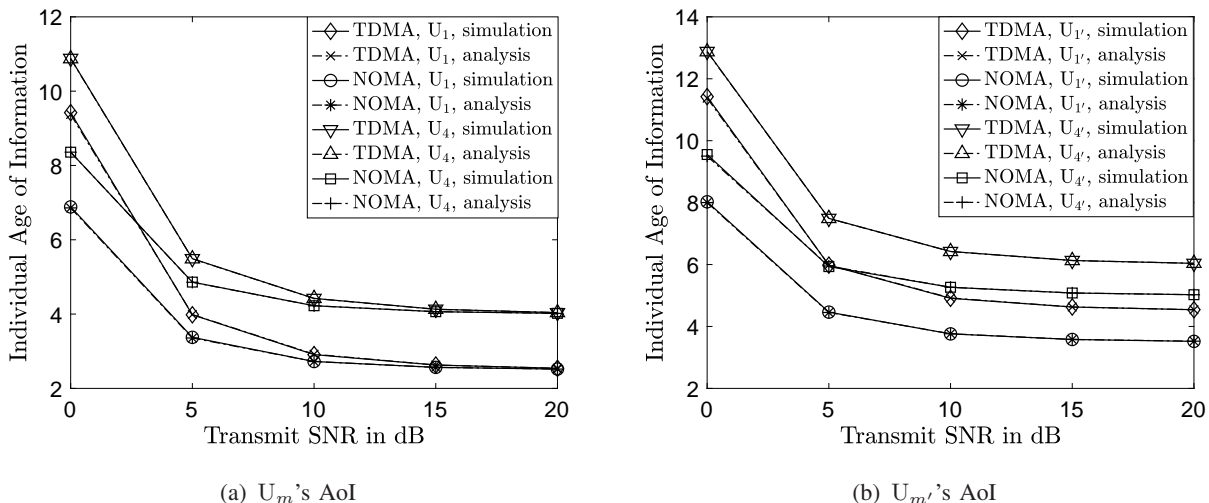


Fig. 7. The impact of NOMA transmission on the individual AoI for the generate-at-request model with $M = 8$, $R = 1$ bit/s/Hz and $T = 0.5$ s.

In Fig. 6, the impact of the number of users, M , on the AoI achieved by the considered transmission protocols is studied. As can be seen from the figure, by increasing M , the AoI is increased for both transmission protocols. This observation is expected since with more users in the network, each user has to wait for a longer period of time to be served. In addition, one can also observe that the performance gain of the proposed NOMA protocol over TDMA increases as the number of users, M , increases. For example, the performance gap between the two protocols is 5 for $M = 8$, and increases to 25 for $M = 32$. This observation means that the proposed NOMA protocol is particularly useful for reducing the AoI of networks with massive connectivity, which is a key use case of the 6G system.

B. The Generate-at-Request Model

Recall that for the GAR model, each user generates its update at the beginning of each TDMA frame, instead of each time slot as in the GAW case. In Fig. 7, the impact of the NOMA transmission protocol on the users' individual AoI is studied for the GAR model. In particular, Fig. 7(a) focuses on U_m 's individual AoI achieved by the two considered transmission protocols, $1 \leq m \leq \frac{M}{2}$. Unlike for the GAW model, different users experience different AoIs for the GAR model, i.e., U_m 's AoI is larger than that of U_i 's, $m > i$. This observation is expected since U_m 's instantaneous AoI can drop to mT at most, whereas U_i 's instantaneous AoI can drop to iT . Fig. 7(a) also shows that for U_m , the performance gain of NOMA over TDMA is similar to that for the GRW case, e.g., the use of NOMA yields a significant performance gain at low SNR but achieves the same AoI as TDMA at high SNR. This performance gain at low SNR is due to the

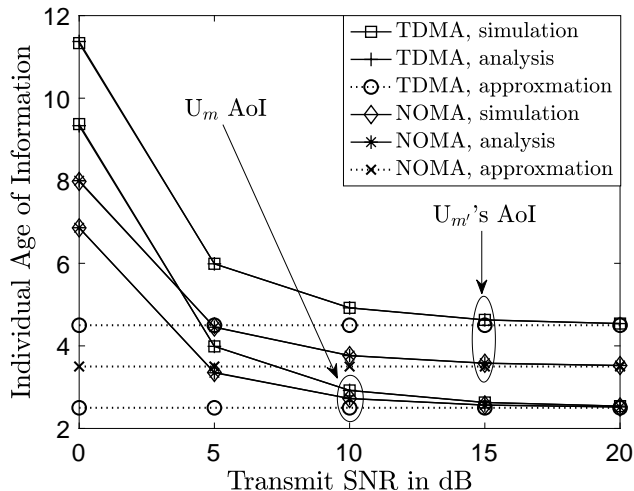


Fig. 8. Comparison of the AoI experienced by U_m and $U_{m'}$, where the generate-at-request model is used, $m = 1$, $M = 8$, $R = 1$ bit/s/Hz and $T = 0.5$ s.

fact that U_m has a second chance for transmission in each frame, whereas for TDMA, U_m has to rely on a single time slot for its updates.

Fig. 7(b) focuses on $U_{m'}$'s individual AoI achieved for the two transmission protocols. As can be seen from the figure, NOMA outperforms TDMA in all SNR regimes. The reason for this superior performance can be explained as follows. Recall that for TDMA, $U_{m'}$ has to rely on the m' -th time slot only for sending its update to the base station. The use of the proposed NOMA protocol has two advantages for reducing the AoI. One is that the use of NOMA offers the user two chances to transmit in each TDMA time frame. The other is that the proposed NOMA protocol can schedule $U_{m'}$ to transmit earlier, i.e., completing its update in the m -th time slot, instead of waiting for the m' -th time slot as for TDMA. The latter is crucial for NOMA to outperform TDMA in the high SNR regime, as indicated by Corollary 2. Furthermore, we note that the subfigures of Fig. 7 demonstrate the accuracy of the developed analytical results shown in Lemma 2.

In Fig. 8, the individual AoI experienced by U_m and $U_{m'}$ is compared. As can be seen from the figure, for the TDMA transmission protocol, $U_{m'}$'s AoI is much larger than that of U_m , which is due to the fact that $U_{m'}$ has to wait for the m' -th time slot to deliver its update and hence experiences large access delays. By using the proposed NOMA protocol, the difference between the two users' AoI can be reduced significantly. For example, at high SNR, the difference between the two users' AoI is 2 with TDMA, and can be halved by applying NOMA. Therefore, the use of NOMA can effectively reduce the difference between the users' AoI and hence improve user

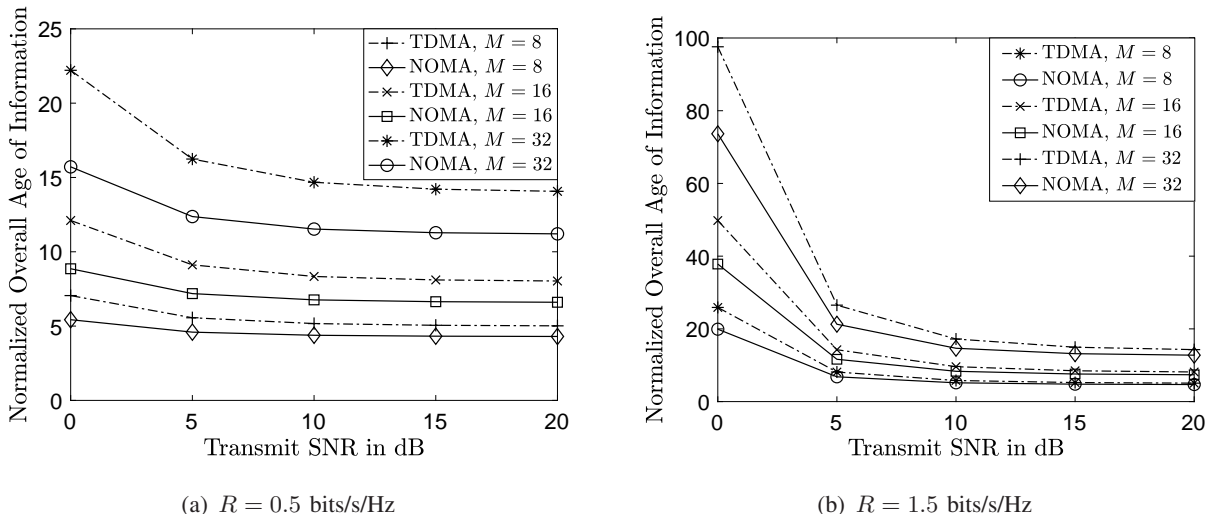


Fig. 9. The impact of NOMA transmission on the overall AoI, where the generate-at-request model is used and $T = 0.5$ s.

fairness, as discussed in Remark 4. We also note that Fig. 8 demonstrates the accuracy of the high SNR approximations developed in Section IV-B.

In Fig. 9, the normalized overall AoI is used as the metric to study the performance of the proposed NOMA transmission protocol with the GAR model. We note that for the GAW model, the proposed NOMA protocol has the limitation that it can outperform TDMA in the low SNR regime only, as shown in Figs. 5 and 6. Compared to Figs. 5 and 6, Fig. 9 shows that the proposed NOMA protocol can always outperform TDMA and realize a smaller overall AoI in all SNR regimes. The performance gain of NOMA over TDMA is significant for small R , and is reduced by increasing R , as shown in the two subfigures of Fig. 9. Furthermore, Fig. 9 also demonstrates that the performance gain of NOMA over TDMA increases as the number of the users, M , increases, which is consistent with the observations related to Fig. 6.

VI. CONCLUSIONS

In this paper, NOMA has been used as an add-on to reduce the AoI of a legacy TDMA network. By using the key features of the two considered data generation models, namely GAW and GAR, two CR-NOMA transmission protocols have been developed to reduce the AoI of the network. Closed-form expressions of the AoI achieved by the proposed NOMA protocols have been derived, and an asymptotic analysis has been carried out to show that the use of NOMA can reduce the AoI due to the following two reasons. First, the use of NOMA provides users more chances to transmit, which ensures that the users can update their base station more frequently. Second, the use of NOMA allows the users to transmit earlier than in the TDMA

case, and hence, improve the freshness of the data available at the base station. In this paper, it was assumed that the signals of the secondary users are decoded first at the base station before decoding the primary users' signals. The use of more dynamic SIC decoding orders can potentially lead to a larger AoI reduction, which is an important direction for future research. In addition, in this paper, the users' CSI is assumed to be perfectly known for the implementation of NOMA. An important future research direction is to study the impact of imperfect CSI on the AoI reduction.

APPENDIX A

PROOF FOR LEMMA 1

It is straightforward to verify that all the users experience the same AoI with CR-NOMA for the GAW case, and therefore, U_m 's AoI is considered in the remainder of this proof. Unlike the case of TDMA, the duration between the beginning and the end of the j -th successful update is not always a multiple of MT , since each user has two chances to transmit in each frame. For illustration, assume that U_m 's $(j - 1)$ -th successful update finishes in the i -th frame. Because U_m has two chances to transmit in each frame, the following two events are defined based on which of the two time slots is used:

$$\begin{aligned}
 E_{jm} &= \{\text{the } (j - 1)\text{-th successful update finishes at the end} \\
 &\quad \text{of the } m\text{-th time slot of a frame, e.g., at } t_i^{m+1}\}, \\
 E_{jm'} &= \{\text{the } (j - 1)\text{-th successful update finishes at the end} \\
 &\quad \text{of the } m'\text{-th time slot of a frame, e.g., at } t_i^{m'+1}\}.
 \end{aligned} \tag{22}$$

Denote the time interval between the $(j - 1)$ -th and the j -th successful updates by y_j , $j \geq 1$, whose value can be obtained considering by the following four cases:

$$y_j = \begin{cases} x_j MT, & \text{from } t_i^{m+1} \text{ to } x_j MT + t_i^{m+1} \\
 x_j MT, & \text{from } t_i^{m'+1} \text{ to } x_j MT + t_i^{m'+1} \\
 x_j MT + \frac{M}{2}T, & \text{from } t_i^{m+1} \text{ to } x_j MT + \frac{M}{2}T + t_i^{m+1} \\
 x_j MT - \frac{M}{2}T, & \text{from } t_i^{m'+1} \text{ to } x_j MT - \frac{M}{2}T + t_i^{m'+1} \end{cases}, \tag{23}$$

where x_j is defined as the number of frames between the $(j - 1)$ -th and the j -th successful updates, $x_j \in \mathbb{Z}$, and \mathbb{Z} denotes the integer set.

Eq. (23) shows that $y_j = x_j MT$ is caused by two different events. One is that, conditioned on E_{jm} , the user fails to update the base station during the first $(x_j - 1)$ frames, but successfully sends an update in the m -th time slot of the $(x_j + i)$ -th frame, where the user's $(j - 1)$ -th successful update is assumed to occur in the i -th frame without loss of generality. The other is that, conditioned on $E_{jm'}$, the user fails to update the base station during the first $(x_j - 1)$ frames, but successfully sends an update in the m' -th time slot of the $(x_j + i)$ -th frame. $y_j = x_j MT + \frac{M}{2}T$ corresponds to the event that, conditioned on E_{jm} , the user fails to update the base station until the m' -th time slot of the $(x_j + i)$ -th frame. $y_j = x_j MT - \frac{M}{2}T$ corresponds to the event that, conditioned on $E_{jm'}$, the user fails to update the base station until the m -th time slot of the $(x_j + i)$ -th frame. Following the definition of y_j in (23), the following four conditional probabilities can be defined: $p_{j1} = \mathbb{P}(y_j = x_j MT | E_{jm})$, $p_{j2} = \mathbb{P}(y_j = x_j MT + \frac{M}{2}T | E_{jm})$, $p_{j3} = \mathbb{P}(y_j = x_j MT | E_{jm'})$, and $p_{j4} = \mathbb{P}(y_j = x_j MT - \frac{M}{2}T | E_{jm'})$, which will be evaluated later.

U_m 's average AoI achieved by NOMA can be expressed as follows:

$$\begin{aligned} \bar{\Delta}_m^N &= \lim_{J \rightarrow \infty} \frac{\sum_{j=1}^J Q_j}{\sum_{j=1}^J y_j} \\ &= \lim_{J \rightarrow \infty} \frac{\sum_{j=1}^J T y_j + \frac{1}{2} y_j^2}{\sum_{j=1}^J y_j} = T + \frac{1}{2} \frac{\mathcal{E}\{Y^2\}}{\mathcal{E}\{Y\}}, \end{aligned} \quad (24)$$

where $\mathcal{E}\{Y\} = \lim_{J \rightarrow \infty} \frac{1}{J} \sum_{j=1}^J y_j$ and $\mathcal{E}\{Y^2\} = \lim_{J \rightarrow \infty} \frac{1}{J} \sum_{j=1}^J y_j^2$. The remainder of the proof is to evaluate $\mathcal{E}\{Y\}$ and $\mathcal{E}\{Y^2\}$.

Define p_0 as the probability of the event that U_m fails to deliver an update in both of the two time slots in one frame. Note that, in the two time slots, U_m assumes different roles for transmission, i.e., U_m is the primary user in the m -th time slot and the secondary user in the m' -th time slot. By using the data rate constraint in (3) and the assumption that the users' channel gains are i.i.d. complex Gaussian distributed, the probability, p_0 , can be obtained as follows:

$$p_0 = \mathbb{P} \left(\log(1 + P|h_m^{i,m}|^2) \leq \frac{N}{T}, \log \left(1 + \frac{P^S |h_m^{i,m'}|^2}{P|h_m^{i,m'}|^2 + 1} \right) \leq \frac{N}{T} \right) = \left(1 - e^{-\frac{\epsilon}{P^S}} \right) \left(1 - \frac{e^{-\frac{\epsilon}{P^S}}}{1 + \frac{P\epsilon}{P^S}} \right),$$

where the channel gains in the i -th frame are used for illustrative purposes.

Denote the probability for the user to successfully deliver its update in the m -th time slot by p_m , which can be expressed as follows:

$$p_m = \mathbb{P} \left(\log(1 + P^S |h_m^{i,m}|^2) \geq \frac{N}{T} \right) = e^{-\frac{\epsilon}{P^S}}. \quad (25)$$

Denote the probability for the event that the user fails to deliver its update in the m -th time slot but successfully delivers a new update in the m' -th time slot by $p_{m'}$. This probability can be expressed as follows:

$$\begin{aligned} p_{m'} &= \mathbb{P} \left(\log(1 + P|h_m^{i,m}|^2) \leq \frac{N}{T}, \log \left(1 + \frac{PS|h_m^{i,m'}|^2}{P|h_m^{i,m'}|^2 + 1} \right) \geq \frac{N}{T} \right) \\ &= \left(1 - e^{-\frac{\epsilon}{PS}} \right) e^{-\frac{\epsilon}{PS}} \frac{1}{1 + \frac{P\epsilon}{PS}}. \end{aligned}$$

Therefore, $\mathcal{E}\{Y\}$ can be obtained as follows:

$$\begin{aligned} \mathcal{E}\{Y\} &= \sum_{x_j \in \mathbb{Z}} x_j MT (p_{j1} \mathbb{P}(E_{jm}) + p_{j3} \mathbb{P}(E_{jm'})) + \sum_{x_j \in \mathbb{Z}} \left(x_j MT + \frac{M}{2} T \right) p_{j2} \mathbb{P}(E_{jm}) \quad (26) \\ &\quad + \sum_{x_j \in \mathbb{Z}} \left(x_j MT - \frac{M}{2} T \right) p_{j4} \mathbb{P}(E_{jm'}) \\ &= \sum_{j=1}^{\infty} j MT (p_0^{j-1} p_m^2 + p_0^{j-1} p_{m'}^2) + \sum_{j=1}^{\infty} \left(j MT + \frac{M}{2} T \right) p_0^{j-1} p_m p_{m'} \\ &\quad + \sum_{j=1}^{\infty} \left(j MT - \frac{M}{2} T \right) p_0^{j-1} p_m p_{m'}, \end{aligned}$$

where the last step is obtained by using the following facts: $\mathbb{P}(E_{jm}) = p_m$, $\mathbb{P}(E_{jm'}) = p_{m'}$, $p_{j1} = p_0^{j-1} p_m$, $p_{j2} = p_0^{j-1} p_{m'}$, $p_{j3} = p_0^{j-1} p_{m'}$, and $p_{j4} = p_0^{j-1} p_m$. With some straightforward algebraic manipulations, the expression of $\mathcal{E}\{Y\}$ can be simplified as follows:

$$\begin{aligned} \mathcal{E}\{Y\} &= MT(p_m^2 + p_{m'}^2 + 2p_m p_{m'}) p_0^{-1} \sum_{j=1}^{\infty} j p_0^j \quad (27) \\ &= MT(p_m + p_{m'})^2 \frac{1}{(1 - p_0)^2}, \end{aligned}$$

where the last step follows from the following infinite sum of series:

$$\sum_{j=1}^{\infty} j x^j = x \sum_{j=1}^{\infty} \frac{d}{dx} x^j = x \frac{d}{dx} \sum_{j=1}^{\infty} x^j = \frac{x}{(1-x)^2}. \quad (28)$$

for $0 < x < 1$.

On the other hand, $\mathcal{E}\{Y^2\}$ can be obtained as follows:

$$\begin{aligned}
\mathcal{E}\{Y^2\} &= \sum_{j=1}^{\infty} j^2 M^2 T^2 (p_{j1} \mathbb{P}(E_{jm}) + p_{j3} \mathbb{P}(E_{jm'})) + \sum_{j=1}^{\infty} \left(jMT + \frac{M}{2}T \right)^2 p_{j2} \mathbb{P}(E_{jm}) \quad (29) \\
&\quad + \sum_{j=1}^{\infty} \left(jMT - \frac{M}{2}T \right)^2 p_{j4} \mathbb{P}(E_{jm'}) \\
&= \sum_{j=1}^{\infty} j^2 M^2 T^2 (p_0^{j-1} p_m^2 + p_0^{j-1} p_{m'}^2) + \sum_{j=1}^{\infty} \left(jMT + \frac{M}{2}T \right)^2 p_0^{j-1} p_{m'} p_m \\
&\quad + \sum_{j=1}^{\infty} \left(jMT - \frac{M}{2}T \right)^2 p_0^{j-1} p_m p_{m'}.
\end{aligned}$$

With some straightforward algebraic manipulations, the expression of $\mathcal{E}\{Y^2\}$ can be simplified as follows:

$$\begin{aligned}
\mathcal{E}\{Y^2\} &= M^2 T^2 (p_m + p_{m'})^2 p_0^{-1} \sum_{j=1}^{\infty} j^2 p_0^j + \frac{M^2}{2} T^2 p_m p_{m'} p_0^{-1} \sum_{j=1}^{\infty} p_0^j \quad (30) \\
&= M^2 T^2 (p_m + p_{m'})^2 \frac{(1+p_0)}{(1-p_0)^3} + \frac{M^2}{2} T^2 \frac{p_m p_{m'}}{1-p_0},
\end{aligned}$$

where the last step follows from the following infinite sum of series:

$$\sum_{j=1}^{\infty} j^2 x^j = x \sum_{j=1}^{\infty} j \frac{d}{dx} x^j = x \frac{d}{dx} \sum_{j=1}^{\infty} j x^j = \frac{x(1+x)}{(1-x)^3}. \quad (31)$$

Therefore, U_m 's average AoI can be calculated as follows:

$$\begin{aligned}
\bar{\Delta}_m^N &= T + \frac{1}{2} \frac{\mathcal{E}\{Y^2\}}{\mathcal{E}\{Y\}} \quad (32) \\
&= T + \frac{1}{2} \frac{M^2 T^2 (p_m + p_{m'})^2 \frac{(1+p_0)}{(1-p_0)^3} + \frac{M^2}{2} T^2 p_m p_{m'} \frac{1}{1-p_0}}{MT (p_m + p_{m'})^2 \frac{1}{(1-p_0)^2}}.
\end{aligned}$$

By using the fact that all the users experiences the same AoI and with some straightforward algebraic manipulations, the lemma is proved.

APPENDIX B

PROOF FOR LEMMA 2

For the GAR model, different users experience different AoI.s In the proof, the common steps for the analysis of the users' AoIs are provided first and then the specific results for the users' individual AoIs are presented.

A. *Generic Expression for the AoI, $\bar{\Delta}_k^N$, $k \in \{m, m'\}$*

To facilitate the analysis of the AoI, the events in (22) are first modified as follows:

$$\begin{aligned}
 E_{jm}^k &= \{U_k \text{'s } (j-1)\text{-th successful update finishes at the} \\
 &\quad \text{end of the } m\text{-th time slot of a frame, e.g., at } t_i^{m+1}\}, \\
 E_{jm'}^k &= \{U_k \text{'s } (j-1)\text{-th successful update finishes at the} \\
 &\quad \text{end of the } m'\text{-th time slot of a frame, e.g., at } t_i^{m'+1}\}.
 \end{aligned} \tag{33}$$

where $k \in \{m, m'\}$.

Denote by y_{jk} the time interval between U_k 's $(j-1)$ -th and j -th successful updates, $k \in \{m, m'\}$. Depending on which of the two events, E_{jm}^k and $E_{jm'}^k$, happens, the value of y_{jk} will be different. Furthermore, the height of the rectangle in the shaded region shown in Fig. 4 also depends on the two events, E_{jm}^k and $E_{jm'}^k$. For example, U_m 's instantaneous AoI is reset to mT if the user's $(j-1)$ -th successful update finishes in the m -th time slot of the last frame, i.e., E_{jm}^m occurs. If $E_{jm'}^m$ occurs, i.e., the user's $(j-1)$ -th successful update finishes in the m' -th time slot of the last frame, U_m 's AoI is reset to $m'T$. $U_{m'}$'s instantaneous AoI is changed similar to that of U_m 's AoI. Therefore, the average AoI achieved by CR-NOMA can be expressed as follows:

$$\begin{aligned}
 \bar{\Delta}_k^N &= \lim_{J \rightarrow \infty} \frac{\sum_{j=1}^J Q_j^k}{\sum_{j=1}^J y_{jk}} \\
 &= \lim_{J \rightarrow \infty} \frac{\sum_{j=1}^J \left(\mathbf{1}_{E_{jm}^k} mT + \mathbf{1}_{E_{jm'}^k} m'T \right) y_{jk} + \frac{1}{2} y_{jk}^2}{\sum_{j=1}^J y_{jk}},
 \end{aligned} \tag{34}$$

where $k \in \{m, m'\}$, Q_j^k denotes the area of the shaded shape shown in Fig. 4, and $\mathbf{1}_E$ is an indicator function, i.e., $\mathbf{1}_E = 1$ if event E happens, otherwise $\mathbf{1}_E = 0$. By using steps similar to those in the proof of Lemma 1, $\bar{\Delta}_k^N$ can be expressed as follows:

$$\bar{\Delta}_k^N = \Delta_{k,0} + \frac{1}{2} \frac{\mathcal{E}\{Y_k^2\}}{\mathcal{E}\{Y_k\}}, \tag{35}$$

where $\mathcal{E}\{Y_k\} = \lim_{J \rightarrow \infty} \frac{1}{J} \sum_{j=1}^J y_{jk}$, $\mathcal{E}\{Y_k^2\} = \lim_{J \rightarrow \infty} \frac{1}{J} \sum_{j=1}^J y_{jk}^2$, and $\Delta_{k,0}$ is defined as follows:

$$\Delta_{k,0} \triangleq \lim_{J \rightarrow \infty} \frac{\sum_{j=1}^J \left(\mathbf{1}_{E_{jm}^k} mT + \mathbf{1}_{E_{jm'}^k} m'T \right) y_{jk}}{\sum_{j=1}^J y_{jk}}. \tag{36}$$

To facilitate the performance analysis, denote by p_{0k} the probability of the event that U_k fails to deliver an update in both of the two time slots of one frame, by p_{mk} the probability of the

event that U_k successfully delivers its update in the m -th time slot of a frame, and by $p_{m'k}$ the probability of the event that U_k fails in the m -th time slot but successfully delivers its update in the m' -th time slot of the same frame, $k \in \{m, m'\}$.

By using the same steps in Appendix A, it is straightforward to show that the second term in (35) is simply $\Delta(p_{0k}, p_{mk}, p_{m'k})$. Therefore, in the remainder of the proof, we focus on the evaluation of the first term in (35), $\Delta_{k,0}$, as well as the probabilities, p_{0k} , p_{mk} and $p_{m'k}$, as shown in the following sections.

B. Evaluation of $\Delta_{k,0}$, $k \in \{m, m'\}$

By using the expectation $\mathcal{E}\{Y_k\}$, $\Delta_{k,0}$ in (35) can be expressed as follows:

$$\begin{aligned} \Delta_{k,0} &= \lim_{J \rightarrow \infty} \frac{\frac{\sum_{j=1}^J \mathbf{1}_{E_{jm}^k} mTy_{jk}}{J} + \frac{\sum_{j=1}^J \mathbf{1}_{E_{jm'}^k} m'Ty_{jk}}{J}}{\frac{\sum_{j=1}^J y_{jk}}{J}} \quad (37) \\ &= \frac{mT}{\mathcal{E}\{Y_k\}} \lim_{J \rightarrow \infty} \frac{\sum_{j=1}^J \mathbf{1}_{E_{jm}^k}}{J} \frac{\sum_{j=1}^J \mathbf{1}_{E_{jm}^k} y_{jk}}{\sum_{j=1}^J \mathbf{1}_{E_{jm}^k}} + \frac{m'T}{\mathcal{E}\{Y_k\}} \lim_{J \rightarrow \infty} \frac{\sum_{j=1}^J \mathbf{1}_{E_{jm'}^k}}{J} \frac{\sum_{j=1}^J \mathbf{1}_{E_{jm'}^k} y_{jk}}{\sum_{j=1}^J \mathbf{1}_{E_{jm'}^k}}. \end{aligned}$$

Define the following two conditional expectations: $\mathcal{E}\{Y_k|E_{jm}^k\} = \lim_{J \rightarrow \infty} \frac{\sum_{j=1}^J \mathbf{1}_{E_{jm}^k} mTy_{jk}}{\sum_{j=1}^J \mathbf{1}_{E_{jm}^k}}$ and $\mathcal{E}\{Y_k|E_{jm'}^k\} = \lim_{J \rightarrow \infty} \frac{\sum_{j=1}^J \mathbf{1}_{E_{jm'}^k} m'Ty_{jk}}{\sum_{j=1}^J \mathbf{1}_{E_{jm'}^k}}$, which can be used to simplify the expression for $\Delta_{k,0}$ as follows:

$$\Delta_{k,0} = \frac{mT\mathbb{P}(E_{jm}^k)\mathcal{E}\{Y_k|E_{jm}^k\} + m'T\mathbb{P}(E_{jm'}^k)\mathcal{E}\{Y_k|E_{jm'}^k\}}{\mathcal{E}\{Y_k\}}. \quad (38)$$

For illustrative purposes, assume that U_k 's $(j-1)$ -th successful update happens in the i -th frame. Therefore, E_{jm}^k means that U_k 's $(j-1)$ -th successful update happens in the m -th time slot of the i -th frame, and hence y_{jk} can have the following two forms:

$$y_{jk} = \begin{cases} x_{jk}MT, & \text{from } t_i^{m+1} \text{ to } x_{jk}MT + t_i^{m+1} \\ x_{jk}MT + \frac{M}{2}T, & \text{from } t_i^{m+1} \text{ to } x_{jk}MT + \frac{M}{2}T + t_i^{m+1}, \end{cases} \quad (39)$$

where x_{jk} denotes the number of frames between U_k 's $(j-1)$ -th and j -th successful updates. Therefore, $\mathcal{E}\{Y_k|E_{jm}^k\}$ can be obtained as follows:

$$\mathcal{E}\{Y_k|E_{jm}^k\} = \sum_{x_{jk} \in \mathbb{Z}} x_{jk}MT p_{j1}^k + \sum_{x_{jk} \in \mathbb{Z}} \left(x_{jk}MT + \frac{M}{2}T \right) p_{j2}^k, \quad (40)$$

where $p_{j1}^k = \mathbb{P}(y_{jk} = x_{jk}MT|E_{jm}^k)$ and $p_{j2}^k = \mathbb{P}(y_{jk} = x_{jk}MT + \frac{M}{2}T|E_{jm}^k)$, for $k \in \{m, m'\}$.

By using the fact that the users' channel gains in different time slots are i.i.d., the conditional expectation, $\mathcal{E}\{Y_k|E_{jm}^k\}$, can be rewritten as follows:

$$\begin{aligned}\mathcal{E}\{Y_k|E_{jm}^k\} &\stackrel{(1)}{=} \sum_{j=1}^{\infty} jMT p_{0k}^{j-1} p_{mk} + \sum_{j=1}^{\infty} \left(jMT + \frac{M}{2}T \right) p_{0k}^{j-1} p_{m'k} \\ &\stackrel{(2)}{=} \frac{MT(p_{mk} + p_{m'k})}{(1-p_{0k})^2} + \frac{1}{2} \frac{MT p_{m'k}}{1-p_{0k}},\end{aligned}\quad (41)$$

where the first step follows from $p_{j1}^k = p_{0k}^{j-1} p_{mk}$ and $p_{j2}^k = p_{0k}^{j-1} p_{m'k}$, and the last step follows by using (28) and (31).

On the other hand, conditioned on $E_{jm'}^k$, y_{jk} can have the following two forms:

$$y_{jk} = \begin{cases} x_{jk}MT, & \text{from } t_i^{m'+1} \text{ to } x_{jk}MT + t_i^{m'+1} \\ x_{jk}MT - \frac{M}{2}T, & \text{from } t_i^{m'+1} \text{ to } x_{jk}MT - \frac{M}{2}T + t_i^{m'+1}. \end{cases}\quad (42)$$

Based on the above options for y_{jk} , the conditional expectation, $\mathcal{E}\{Y_k|E_{jm'}^k\}$, can be obtained as follows:

$$\begin{aligned}\mathcal{E}\{Y_k|E_{jm'}^k\} &= \sum_{x_{jk} \in \mathbb{Z}} x_{jk}MT p_{j3}^k + \sum_{x_{jk} \in \mathbb{Z}} \left(x_{jk}MT - \frac{M}{2}T \right) p_{j4}^k \\ &= \sum_{j=1}^{\infty} jMT p_{0k}^{j-1} p_{m'k} + \sum_{j=1}^{\infty} \left(jMT - \frac{M}{2}T \right) p_{0k}^{j-1} p_{mk} \\ &= \frac{MT(p_{mk} + p_{m'k})}{(1-p_{0k})^2} - \frac{1}{2} \frac{MT p_{mk}}{1-p_{0k}},\end{aligned}\quad (43)$$

where $p_{j3}^k \triangleq \mathbb{P}(y_{jk} = x_{jk}MT | E_{jm'}^k) = p_{0k}^{j-1} p_{m'k}$, and $p_{j4}^k \triangleq \mathbb{P}(y_{jk} = x_{jk}MT - \frac{M}{2}T | E_{jm'}^k) = p_{0k}^{j-1} p_{mk}$.

By using the two conditional expectations, $\Delta_{k,0}$ can be obtained as follows:

$$\begin{aligned}\Delta_{k,0} &\stackrel{(1)}{=} \frac{mT \mathbb{P}(E_{jm}^k) \mathcal{E}\{Y_k|E_{jm}^k\} + m'T \mathbb{P}(E_{jm'}^k) \mathcal{E}\{Y_k|E_{jm'}^k\}}{\mathcal{E}\{Y_k\}} \\ &\stackrel{(2)}{=} \frac{mT p_{mk} \mathcal{E}\{Y_k|E_{jm}^k\} + m'T p_{m'k} \mathcal{E}\{Y_k|E_{jm'}^k\}}{\mathcal{E}\{Y_k\}} \\ &\stackrel{(3)}{=} \frac{1}{(p_{mk} + p_{m'k})^2 \frac{1}{(1-p_{0k})^2}} \left[\left((p_{mk} + p_{m'k}) \frac{mT p_{mk}}{(1-p_{0k})^2} + \frac{p_{m'k}}{2} \frac{mT p_{mk}}{1-p_{0k}} \right) \right. \\ &\quad \left. + \left((p_{mk} + p_{m'k}) \frac{m'T p_{m'k}}{(1-p_{0k})^2} - \frac{p_{mk}}{2} \frac{m'T p_{m'k}}{1-p_{0k}} \right) \right],\end{aligned}\quad (44)$$

where the second step follows from the fact that $\mathbb{P}(E_{jm}^k) = p_{mk}$, $\mathbb{P}(E_{jm'}^k) = p_{m'k}$, and the last step follows from the fact that $\mathcal{E}\{Y_k\} = MT(p_{mk} + p_{m'k})^2 \frac{1}{(1-p_{0k})^2}$. As can be seen from the above expression, the first term of the users' AoI expression in (35), $\bar{\Delta}_k^N$, can be explicitly written as

a function of p_{0k} , p_{mk} , and $p_{m'k}$, which will be evaluated in the following two subsections for the two users, respectively.

C. Evaluation of p_{0m} , p_{mm} , and $p_{m'm}$

Recall that p_{0m} is the probability of the event that U_m fails to deliver an update in both of the two time slots of a given frame. Note that in each of the two times slots, U_m is allowed to transmit in different roles. Further note that if the update from $U_{m'}$ in the m -th time slot is successful, $U_{m'}$ will remain silent in the m' -th time slot, which means that U_m solely occupies this time slot. By using the date rate constraint in (3), the probability, p_0 , can be expressed as follows:

$$p_{0m} = \mathbb{P} \left(\log(1 + P|h_m^{i,m}|^2) \leq \frac{N}{T}, \log \left(1 + \frac{P^S|h_{m'}^{i,m}|^2}{P|h_m^{i,m}|^2 + 1} \right) \leq \frac{N}{T}, \log \left(1 + \frac{P^S|h_m^{i,m'}|^2}{P|h_{m'}^{i,m'}|^2 + 1} \right) \leq \frac{N}{T} \right) \\ + \mathbb{P} \left(\log(1 + P|h_m^{i,m}|^2) \leq \frac{N}{T}, \log \left(1 + \frac{P^S|h_{m'}^{i,m}|^2}{P|h_m^{i,m}|^2 + 1} \right) \geq \frac{N}{T}, \log \left(1 + P^S|h_m^{i,m'}|^2 \right) \leq \frac{N}{T} \right), \quad (45)$$

where the i -th frame is used for illustration.

Because the users' channel gains in different time slots are assumed to be independent, the event $E_1 \triangleq \left\{ \log(1 + P|h_m^{i,m}|^2) \leq \frac{N}{T}, \log \left(1 + \frac{P^S|h_{m'}^{i,m}|^2}{P|h_m^{i,m}|^2 + 1} \right) \leq \frac{N}{T} \right\}$ is independent from the event $\left\{ \log \left(1 + \frac{P^S|h_m^{i,m'}|^2}{P|h_{m'}^{i,m'}|^2 + 1} \right) \leq \frac{N}{T} \right\}$. Therefore, the probability of E_1 can be calculated separately as follows:

$$\mathbb{P}(E_1) = \mathbb{P} \left(P|h_m^{i,m}|^2 \leq \epsilon, \frac{P^S|h_{m'}^{i,m}|^2}{P|h_m^{i,m}|^2 + 1} \leq \epsilon \right) \quad (46) \\ = \int_0^{\frac{\epsilon}{P}} \left(1 - e^{-\frac{\epsilon}{P^S}(Px+1)} \right) e^{-x} dx = 1 - e^{-\frac{\epsilon}{P}} - e^{-\frac{\epsilon}{P^S}} \frac{1 - e^{-\left(\frac{\epsilon}{P^S}P+1\right)\frac{\epsilon}{P}}}{\frac{\epsilon}{P^S}P + 1}.$$

Similarly define $E_2 \triangleq \left\{ \log(1 + P|h_m^{i,m}|^2) \leq \frac{N}{T}, \log \left(1 + \frac{P^S|h_{m'}^{i,m}|^2}{P|h_m^{i,m}|^2 + 1} \right) \geq \frac{N}{T} \right\}$. The probability of E_2 can be evaluated as follows:

$$\mathbb{P}(E_2) = \mathbb{P} \left(P|h_m^{i,m}|^2 \leq \epsilon, \frac{P^S|h_{m'}^{i,m}|^2}{P|h_m^{i,m}|^2 + 1} \geq \epsilon \right) \quad (47) \\ = e^{-\frac{\epsilon}{P^S}} \frac{1 - e^{-\left(\frac{\epsilon}{P^S}P+1\right)\frac{\epsilon}{P}}}{\frac{\epsilon}{P^S}P + 1}.$$

By substituting (46) and (47) into (45) and with some algebraic manipulations, probability p_{0m} can be expressed as follows:

$$p_{0m} = \left(1 - e^{-\frac{\epsilon}{P}} - e^{-\frac{\epsilon}{P^S}} \frac{1 - e^{-\left(\frac{\epsilon}{P^S}P+1\right)\frac{\epsilon}{P}}}{\frac{\epsilon}{P^S}P + 1} \right) \left(1 - \frac{e^{-\frac{\epsilon}{P^S}}}{1 + \frac{P\epsilon}{P^S}} \right) + e^{-\frac{\epsilon}{P^S}} \frac{1 - e^{-\left(\frac{\epsilon}{P^S}P+1\right)\frac{\epsilon}{P}}}{\frac{\epsilon}{P^S}P + 1} \left(1 - e^{-\frac{\epsilon}{P^S}} \right).$$

Recall that $p_{m'm}$ is the probability for the event that the user fails to deliver its update in the m -th time slot but successfully delivers the update in the m' -th time slot. This probability can be expressed as follows:

$$\begin{aligned} p_{m'm} &= \mathbb{P} \left(\log(1 + P|h_m^{i,m}|^2) \leq \frac{N}{T}, \log \left(1 + \frac{PS|h_m^{i,m}|^2}{P|h_m^{i,m}|^2 + 1} \right) \leq \frac{N}{T}, \log \left(1 + \frac{PS|h_m^{i,m'}|^2}{P|h_m^{i,m'}|^2 + 1} \right) \geq \frac{N}{T} \right) \\ &\quad + \mathbb{P} \left(\log(1 + P|h_m^{i,m}|^2) \leq \frac{N}{T}, \log \left(1 + \frac{PS|h_m^{i,m'}|^2}{P|h_m^{i,m'}|^2 + 1} \right) \geq \frac{N}{T}, \log(1 + PS|h_m^{i,m'}|^2) \geq \frac{N}{T} \right) \\ &= \left(1 - e^{-\frac{\epsilon}{P}} - e^{-\frac{\epsilon}{PS}} \frac{1 - e^{-\left(\frac{\epsilon}{PS}P+1\right)\frac{\epsilon}{P}}}{\frac{\epsilon}{PS}P + 1} \right) e^{-\frac{\epsilon}{PS}} \frac{1}{1 + \frac{P\epsilon}{PS}} + e^{-\frac{2\epsilon}{PS}} \frac{1 - e^{-\left(\frac{\epsilon}{PS}P+1\right)\frac{\epsilon}{P}}}{\frac{\epsilon}{PS}P + 1}, \end{aligned}$$

where the last step is obtained by following steps similar to those for evaluating p_{0m} . It is straightforward to show that $p_{mm} = p_m$.

By substituting the expressions of p_{0m} , p_{mm} , $p_{m'm}$ and $\Delta_{m,0}$ in (35), a closed-form expression for U_m 's AoI can be obtained as shown in the lemma.

D. Evaluation of $p_{0m'}$, $p_{mm'}$ and $p_{m'm'}$

Recall that $p_{0m'}$ is the probability of the event that $U_{m'}$ fails to deliver an update in one frame. Again, we take the i -th frame as an example. Note that $U_{m'}$ is the secondary user in the m -th time slot and the primary user in the m' -th time slot, which means that $p_{0m'}$ can be expressed as follows:

$$p_{0m'} = \mathbb{P} \left(\log \left(1 + \frac{PS|h_{m'}^{i,m}|^2}{P|h_{m'}^{i,m}|^2 + 1} \right) \leq \frac{N}{T}, \log(1 + P|h_{m'}^{i,m'}|^2) \leq \frac{N}{T} \right). \quad (48)$$

It is interesting to observe that the expression for $p_{0m'}$ is simpler than that for p_{0m} in (45) because $U_{m'}$ is the primary user in the m' -th time slot and its data rate in this time slot is always $\log(1 + P|h_{m'}^{i,m'}|^2)$, regardless of U_m 's transmission strategy in the m' -th time slot.

By using the assumption that the users' channels are i.i.d. Rayleigh faded, $p_{0m'}$ can be evaluated as follows:

$$\begin{aligned} p_{0m'} &= \mathbb{P} \left(\frac{PS|h_{m'}^{i,m}|^2}{P|h_{m'}^{i,m}|^2 + 1} \leq \epsilon \right) \mathbb{P} \left(|h_{m'}^{i,m'}|^2 \leq \frac{\epsilon}{P} \right) \\ &= \left(1 - e^{-\frac{\epsilon}{PS}} \frac{1}{1 + \frac{\epsilon P}{PS}} \right) (1 - e^{-\frac{\epsilon}{P}}). \end{aligned} \quad (49)$$

Recall that $p_{mm'}$ denotes the probability of the event that $U_{m'}$ successfully delivers its update in the m -th time slot of a frame, which can be expressed as follows:

$$\begin{aligned} p_{mm'} &= \mathbb{P} \left(\log \left(1 + \frac{P^S |h_{m'}^{i,m}|^2}{P |h_m^{i,m}|^2 + 1} \right) \geq \frac{N}{T} \right) \\ &= e^{-\frac{\epsilon}{PS}} \frac{1}{1 + \frac{\epsilon P}{PS}}. \end{aligned} \quad (50)$$

Recall that $p_{m'm'}$ denotes the probability of the event that $U_{m'}$ fails in the m -th time slot but successfully delivers the update in the m' -th time slot. This probability can be expressed as follows:

$$\begin{aligned} p_{m'm'} &= \mathbb{P} \left(\log \left(1 + \frac{P^S |h_{m'}^{i,m}|^2}{P |h_m^{i,m}|^2 + 1} \right) \leq \frac{N}{T}, \log \left(1 + P |h_{m'}^{i,m'}|^2 \right) \geq \frac{N}{T} \right) \\ &= \left(1 - e^{-\frac{\epsilon}{PS}} \frac{1}{1 + \frac{\epsilon P}{PS}} \right) e^{-\frac{\epsilon}{P}}. \end{aligned} \quad (51)$$

By using the expressions for $p_{0m'}$, $p_{mm'}$, and $p_{m'm'}$, a closed-form expression for $U_{m'}$'s AoI can be obtained as shown in the lemma. This completes the proof.

REFERENCES

- [1] Y. Sun, E. Uysal-Biyikoglu, R. D. Yates, C. E. Koksal, and N. B. Shroff, "Update or wait: How to keep your data fresh," *IEEE Trans. Inform. Theory*, vol. 63, no. 11, pp. 7492–7508, Nov. 2017.
- [2] S. Kaul, R. Yates, and M. Gruteser, "Real-time status: How often should one update?" in *Proc. IEEE INFOCOM*, Orlando, FL, USA, May 2012.
- [3] M. A. Abd-Elmagid, N. Pappas, and H. S. Dhillon, "On the role of age of information in the Internet of Things," *IEEE Commun. Mag.*, vol. 57, no. 12, pp. 72–77, Dec. 2019.
- [4] X. Wu, J. Yang, and J. Wu, "Optimal status update for age of information minimization with an energy harvesting source," *IEEE Trans. Green Commun. and Net.*, vol. 2, no. 1, pp. 193–204, Mar. 2018.
- [5] R. D. Yates, Y. Sun, D. R. Brown, S. K. Kaul, E. Modiano, and S. Ulukus, "Age of information: An introduction and survey," *IEEE J. Sel. Areas Commun.*, vol. 39, no. 5, pp. 1183–1210, May 2021.
- [6] X. You, C. Wang, J. Huang *et al.*, "Towards 6G wireless communication networks: Vision, enabling technologies, and new paradigm shifts," *Sci. China Inf. Sci.*, vol. 64, no. 110301, pp. 1–74, Feb. 2021.
- [7] Z. Zhang, Y. Xiao, Z. Ma, M. Xiao, Z. Ding, X. Lei, G. K. Karagiannidis, and P. Fan, "6G wireless networks: Vision, requirements, architecture, and key technologies," *IEEE Veh. Tech. Mag.*, vol. 14, no. 3, pp. 28–41, Jul. 2019.
- [8] I. Krikidis, "Average age of information in wireless powered sensor networks," *IEEE Wireless Commun. Lett.*, vol. 8, no. 2, pp. 628–631, Apr. 2019.
- [9] A. A. Al-Habob, O. A. Dobre, and H. V. Poor, "Age- and correlation-aware information gathering," *IEEE Wireless Commun. Lett.*, vol. 11, no. 2, pp. 273–277, Feb. 2022.
- [10] M. Xie, J. Gong, S. Cai, and X. Ma, "Age-energy tradeoff for two-hop status update systems with heterogeneous truncated ARQ," *IEEE Wireless Commun. Lett.*, vol. 10, no. 7, pp. 1488–1492, Jul. 2021.

- [11] Y. Zheng, J. Hu, and K. Yang, "Average age of information in wireless powered relay aided communication network," *IEEE Internet of Things Journal*, vol. 9, no. 13, pp. 11 311–11 323, Jul. 2022.
- [12] R. D. Yates and S. K. Kaul, "The age of information: Real-time status updating by multiple sources," *IEEE Trans. Inform. Theory*, vol. 65, no. 3, pp. 1807–1827, Mar. 2019.
- [13] Y. H. Bae and J. W. Baek, "Age of information and throughput in random access-based IoT systems with periodic updating," *IEEE Wireless Commun. Lett.*, vol. 11, no. 4, pp. 821–825, Apr. 2022.
- [14] B. Yu and Y. Cai, "Age of information in grant-free random access with massive MIMO," *IEEE Wireless Commun. Lett.*, vol. 10, no. 7, pp. 1429–1433, Jul. 2021.
- [15] H. Pan and S. C. Liew, "Information update: TDMA or FDMA?" *IEEE Wireless Commun. Lett.*, vol. 9, no. 6, pp. 856–860, Jun. 2020.
- [16] Y. Liu, S. Zhang, X. Mu, Z. Ding, R. Schober, N. Al-Dhahir, E. Hossain, and X. Shen, "Evolution of NOMA toward next generation multiple access (NGMA) for 6G," *IEEE J. Sel. Areas Commun.*, vol. 40, no. 4, pp. 1037–1071, Jan. 2022.
- [17] A. Maatouk, M. Assaad, and A. Ephremides, "Minimizing the age of information: NOMA or OMA?" in *Proc. IEEE INFOCOM WKSHPs*, Paris, France, 2019.
- [18] L. Liu, H. H. Yang, C. Xu, and F. Jiang, "On the peak age of information in NOMA IoT networks with stochastic arrivals," *IEEE Wireless Commun. Lett.*, vol. 10, no. 12, pp. 2757–2761, Dec. 2021.
- [19] H. Zhang, Y. Kang, L. Song, Z. Han, and H. V. Poor, "Age of information minimization for grant-free non-orthogonal massive access using mean-field games," *IEEE Trans. Commun.*, vol. 69, no. 11, pp. 7806–7820, Nov. 2021.
- [20] X. Feng, S. Fu, F. Fang, and F. R. Yu, "Optimizing age of information in RIS-assisted NOMA networks: A deep reinforcement learning approach," *IEEE Wireless Commun. Lett.*, to appear in 2022.
- [21] Z. Gao, A. Liu, C. Han, and X. Liang, "Non-orthogonal multiple access based average age of information minimization in LEO satellite-terrestrial integrated networks," *IEEE Trans. Green Commun. and Net.*, 2022.
- [22] H. Pan, J. Liang, S. C. Liew, V. C. M. Leung, and J. Li, "Timely information update with nonorthogonal multiple access," *IEEE Trans. Industrial Informatics*, vol. 17, no. 6, pp. 4096–4106, Jun. 2021.
- [23] Q. Ren, T.-T. Chan, J. Liang, and H. Pan, "Age of information in sic-based non-orthogonal multiple access," in *Proc. IEEE WCNC*, Austin, TX, USA, 2022.
- [24] Z. Ding, P. Fan, and H. V. Poor, "Impact of user pairing on 5G non-orthogonal multiple access," *IEEE Trans. Veh. Tech.*, vol. 65, no. 8, pp. 6010–6023, Aug. 2016.
- [25] R. E. Kim, J. Li, B. F. J. Spencer, T. Nagayama, and K. A. a. Mechitov, "Synchronized sensing for wireless monitoring of large structures," *Smart Structures and Systems*, vol. 18, no. 5, pp. 885–909, May 2016.
- [26] C. Xu, Q. Xu, J. Wang, K. Wu, K. Lu, and C. Qiao, "AoI-centric task scheduling for autonomous driving systems," in *Proc. IEEE INFOCOM*, London, UK, 2022.